Redox Biology 20 (2019) 107–117

Contents lists available at ScienceDirect

Redox Biology

journal homepage: www.elsevier.com/locate/redox

Research paper

Apoptosis inducing factor deficiency causes retinal photoreceptor degeneration. The protective role of the redox compound methylene blue

Naveen K. Mekala, Jacob Kurdys, Mikayla M. Depuydt, Edwin J. Vazquez, Mariana G. Rosca*

Department of Foundational Sciences at Central Michigan University College of Medicine, Mount Pleasant, MI, United States

ARTICLE INFO

Keywords:
Mitochondria
Complex I
Retina
Photoreceptors
Redox
Methylene blue

ABSTRACT

Dysfunction in mitochondrial oxidative phosphorylation (OXPHOS) underlies a wide spectrum of human ailments known as mitochondrial diseases. Deficiencies in complex I of the electron transport chain (ETC) contribute to 30–40% of all cases of mitochondrial diseases, and leads to eye disease including optic nerve atrophy and retinal degeneration. The mechanisms responsible for organ damage in mitochondrial defects may include energy deficit, oxidative stress, and an increase in the NADH/NAD^+ redox ratio due to decreased NAD^+ regeneration. Currently, there is no effective treatment to alleviate human disease induced by complex I defect.

Photoreceptor cells have the highest energy demand and dependence on OXPHOS for survival, and the lowest reserve capacity indicating that they are sensitive to OXPHOS defects. We investigated the effect of mitochondrial OXPHOS deficiency on retinal photoreceptors in a model of mitochondrial complex I defect (apoptosis inducing factor, AIF-deficient mice, Harlequin mice), and tested the protective effect of a mitochondrial redox compound (methylene blue, MB) on mitochondrial and photoreceptor integrity. MB prevented the reduction in the retinal thickness and protein markers for photoreceptor outer segments, Muller and ganglion cells, and altered mitochondrial integrity and function induced by AIF deficiency. In rotenone-induced complex I deficient 661 W cells (an immortalized mouse photoreceptor cell line) MB decreased the NADH/NAD^+ ratio and oxidative stress without correcting the energy deficit, and improved cell survival. MB deactivated the mitochondrial stress response pathways, the unfolding protein response and mitophagy. In conclusion, preserving mitochondrial structure and function alleviates retinal photoreceptor degeneration in mitochondrial complex I defect.

1. Introduction

The energy necessary for retinal function originates mostly from mitochondrial oxidative phosphorylation (OXPHOS) in which the transport of electrons from respiratory substrates through the electron transport chain (ETC) complexes is coupled with the generation of the inner membrane proton motive force used to generate ATP. As it transfers electrons from NADH to ubiquinone, complex I is the major NADH consumer and NAD^+ generator. Inherited OXPHOS deficiencies cause a large spectrum of human primary mitochondrial diseases of which 30–40% are caused by a complex I defect [1]. An ocular phenotype occurs in approximately 50% of OXPHOS defects in human subjects [2,3]. While missense mutations of mtDNA complex I genes cause retinal ganglion cell death in Leber hereditary optic neuropathy, a disease of the inner retina [4–6], the damage of the outer retina caused by mitochondrial defects has been reported as a rare condition [6]. However, mitochondria are present at the highest density in all outer retinal layers including retinal pigment, photoreceptor [7,8], and Muller glial cells [8], raising the possibility that a decrease in oxidative metabolism is a major pathogenic factor for outer retinal disorders [6].

The Harlequin (Hq) mouse is a model of neuronal degeneration [9] induced by an ecotropic proviral insertion in the intron 1 of the gene encoding Apoptosis Inducing Factor (AIF) leading to decreased AIF protein expression. AIF is a mitochondrial intermembrane space protein [10] that is loosely associated with the inner membrane [11], which promotes apoptosis when translocated to the nucleus [10]. AIF also has cellular functions that are independent from its role in the execution of apoptosis [12–14]. Interestingly, AIF deficiency decreases mitochondrial oxidative phosphorylation (OXPHOS) rates due to a reduced amount of fully assembled complex I [15]. AIF maintains the integrity and mitochondrial import of CHCHD4.1 (Coiled-coil-helix-coiled-coil-helix domain containing 4.1, the human equivalent of the yeast mitochondrial intermembrane space import and assembly protein 40, Mia40/Tim40) that catalyzes oxidative folding and import of OXPHOS

* Correspondence to: Central Michigan University College of Medicine, 2630 Denison Drive, Research Building Room 105, Mount Pleasant, MI 48858, United States.
E-mail address: rosca1g@cmich.edu (M.G. Rosca).

https://doi.org/10.1016/j.redox.2018.09.023
Received 21 August 2018; Received in revised form 25 September 2018; Accepted 27 September 2018
Available online 29 September 2018

protein subunits [16]. Therefore, AIF deficiency causes a posttranslational downregulation of OXPHOS complexes including complex I [1,16–19]. Mice with either a systemic hypomorphic AIF mutation (Hq mice) [9] or tissue-specific AIF knockout [17,18] develop a neuromuscular and retinal mitochondrial cytopathy. In humans, AIF mutations also manifest as familial X-linked mitochondriopathies [20–22]. While retinal ganglion neurons are reported sensitive to the AIF-induced complex I defect [9], its impact on retinal photoreceptors has not been studied.

There is currently no proven treatment to prevent or reverse the retinal degeneration induced by mitochondrial complex I defects. Although oxidative stress is considered a key pathogenic factor for organ damage, antioxidants have shown only modest protective effects in vivo [23,24]. Parallel pathways for electron transport may be induced in mitochondria, and are reported to rescue mitochondrial function in diseases induced by OXPHOS deficiencies. For example, treatment with the coenzyme Q10 derivative idebenone, that shuttles electrons from complex I to complex III, demonstrated promising results in human subjects [25]. A natural homolog of vitamin K rescued pink1 deficient mitochondria—a model of Parkinson's disease—due to its ability to shuttle electrons from complexes I and II to III [26]. The redox compound methylene blue (MB) is reduced by flavin-dependent enzymes (i.e., complex I) to MBH2 whereas cytochrome c is reported to reoxidize MBH2 to MB [27]. Its low redox potential (11 mV) would allow MB to receive electrons from either FMN or Fe-S centers in complex I, and facilitate NADH oxidation. MB is a FDA-approved pharmacological drug that has been used to treat various ailments for more than a century. Chronic administration of low-dose MB enhances memory [28], is neuroprotective against retinal optic neuropathy induced by rotenone-induced complex I inhibition [29], and alleviates cardiac arrest-induced brain damage [30] and neuron loss [31]. It is reported that MB is neuroprotective by normalizing ATP production and decreasing ROS generation [27].

The goals of our study were to establish the value of the Hq mouse in studying complex I-induced degeneration of the outer retina, and determine the therapeutic benefit of a mitochondrial redox compound in protecting the integrity of mitochondria and outer retinal photoreceptor cells. We found that MB prevented the reduction in retinal thickness and the decrease in protein markers for photoreceptor outer segments, Muller and ganglion cells, and preserved mitochondrial integrity and function. In rotenone-induced complex I deficient 661 W cells (immortalized mouse photoreceptor cell line) MB improved cell survival, normalized the NAD^+/NADH ratio and decreased oxidative stress without correcting the energy deficit. MB deactivated the mitochondrial stress response pathways, unfolding protein response and mitophagy.

2. Material and methods

2.1. Animals

Animal experiments were conducted in accordance with the Guide for the Care and Use of Laboratory Animals published by the US National Institutes of Health (NIH Publication No. 85-23, revised 2011), and approved by Central Michigan University Institutional Animal Care and Use Committees. Hemizygous (Hq/Y) males were obtained by mating Hq/X female with Hq/Y males. These mice and their appropriate wild-type controls were obtained from Jackson Laboratory. Mice were housed with a 12-h light-dark cycle, and have free access to food and water. Baldness was assessed as the percentage of the body surface area without hair, and considered a hallmark of the Hq phenotype. To confirm, male mice were genotyped on tail samples as described [1], and phenotyped by determining the AIF protein in retinal homogenates by western blot analyses.

MB shows opposite effects at low versus high doses [32]. Low MB concentrations favor reduction, whereas at higher concentrations MB may “re-route” electrons away from the electron transport chain thus acting as a mitochondrial uncoupler and disrupting the redox balance [33]. For this study MB was administered in drinking water after weaning. Water intake was monitored weekly in order to adjust the MB concentration in drinking water and provide a concentration of MB of 10 mg/kg/day. Our dose selection was based on the reported dose of 1–10 mg/kg in acute intraperitoneal administration that improved memory in mice [34,35]. In our hands, the oral dose of 10 mg/kg improved heart function in a murine model of diabetes [36].

Mice were sacrificed at 11 months of age, and retina were harvested for either immediate or future use (frozen at −80 °C).

2.2. Retinal thickness

Retinas were harvested, fixed and sectioned at 12 μm on a cryostat as described [37]. Formalin-fixed paraffin retinal sections were stained with toluidine blue, and visualized with light microscopy for morphometric studies [38]. Multiple images were taken from the mid-retina and four additional locations (both sides of the optic nerve) at 4×, and the thickness (from the top of the inner nuclear layer to the external side of the pigmental layer) was assessed using a Retiga camera attached to a Nikon Biophot light microscope with Qcapture software (QImaging, Burbay, BC, Canada). Retinal thickness was measured using OpenLab software (Improvision, Lexington, MA). Representative images are shown from the same region, and the average of the five measurements was used for comparison between individual animals.

2.3. Confocal microscopy

Retina cryosections were fixed with pre-cooled acetone, air dried at room temperature, rinsed with 10 mM phosphate buffer, blocked in PBS with 10% FBS, and incubated with primary antibody (dilution 1:500 in PBS with 0.5% BSA) overnight at 4 °C. Retinal sections were probed with fluorescent secondary antibodies (Thermo Fisher) (dilution 10 μg/mL). After washing, slides were air dried, mounted with DAPI (Vector), and examined with a fluorescent microscope. The thickness of the retinal nuclear layers was assessed by measuring the corrected total cell fluorescence (CTCF) as described [39] using Image J (http://rsbweb.nih.gov/ij/download.html).

2.4. Electron microscopy

Posterior eyecups were harvested directly into triple aldehyde-DMSO, sequentially exposed to ferrocyanide-reduced osmium tetroxide and acidified uranyl acetate, dehydrated in ascending concentrations of ethanol, and passed through propylene oxide before being embedded in Poly/Bed resin (Polysciences Inc., 21844-1). Acidified uranyl acetate was used to stain thin sections before examination using a JEOL 1200EX electron microscope. All EM images were independently analyzed, and observed in a blind fashion at the Electron Microscopy Core Facility, Case Western Reserve University. Quantification of the outer segment thickness and damaged mitochondria was performed on EM photographs.

2.5. Cell culture

The photoreceptor-like cells (661 W) were generously provided by Dr. Al-Ubaidi Muayyad from University of Houston, and suspended in growth media conditions as described [40]. Depending upon the experiment, cells were grown in either 35-or 100-mm cell culture dishes, or 96-well culture plates. On attaining confluence, these cells were divided into three experimental groups; control cells, cells treated with rotenone (20 μM), and cells incubated with both rotenone and methylene blue (0-30μM) for 24 h. Cells are harvested and used in various experiments discussed below.

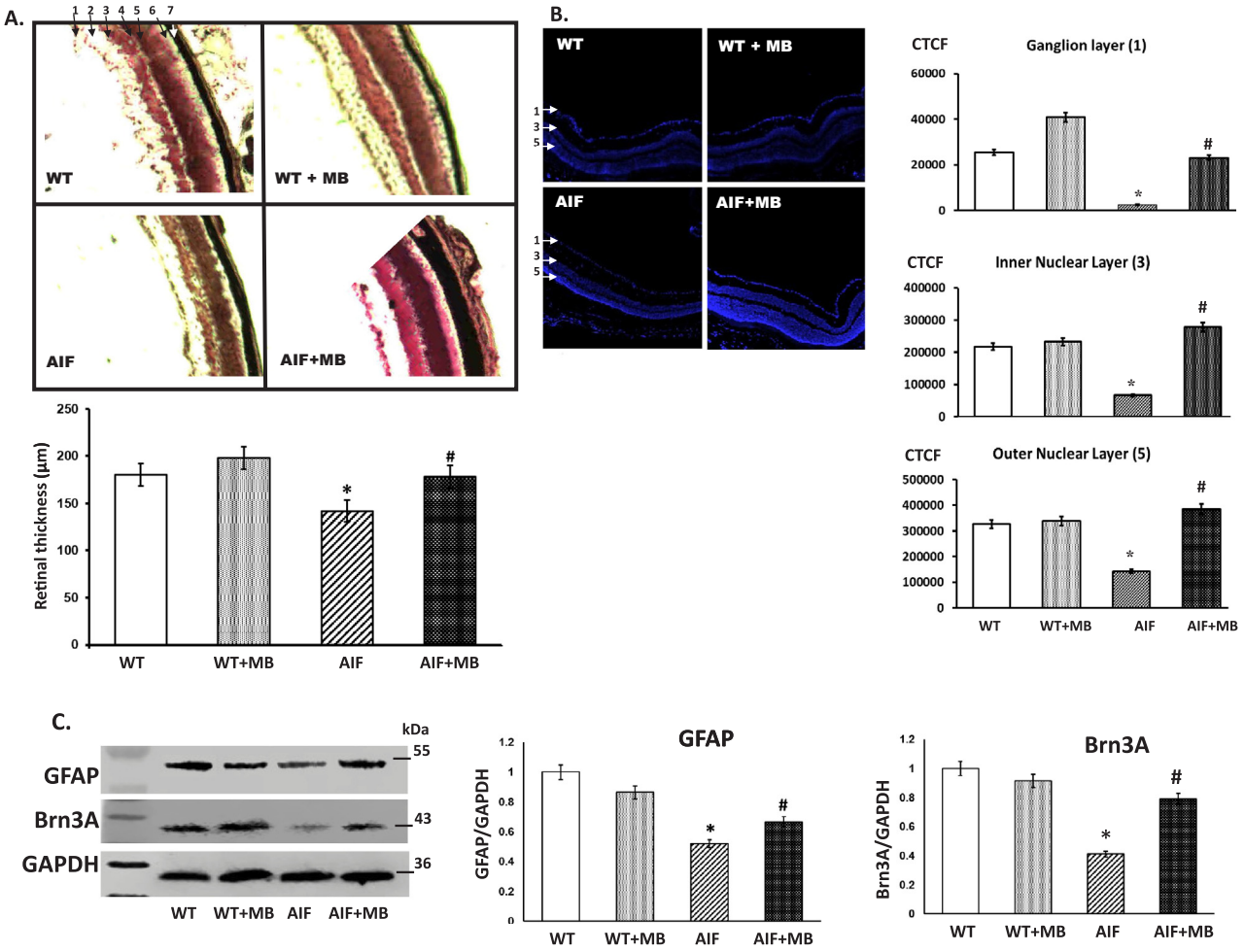

Fig. 1. AIF deficiency causes retinal thinning that is alleviated by methylene blue treatment. A. Light photomicrographs of retinal cryosections (12 μm) stained with toluidine blue from wild type mice (WT), wild type mice treated with methylene blue (WT + MB), AIF deficient mice (AIF), and AIF-deficient mice treated with methylene blue (AIF + MB). The thickness of the retinas was measured, and compared between the groups (lower panel). The numbers represent the retina layers: 1-ganglion; 2-inner plexiform; 3-inner nuclear; 4-outer plexiform; 5-outer nuclear; 6-rod and cone photoreceptor; 7-pigmented epithelium. **B.** Confocal images depicting the retinal cryosection stained with DAPI to show the retinal nuclear layers. The integrity of the ganglion [1], inner nuclear [3] and outer nuclear [5] layers was assessed by measuring the corrected total cell fluorescence (CTCF) on DAPI-stained retinal cryosections as described in the Method section. **C.** Western blot analyses for retinal layer markers. GFAP-Glial fibrillar acidic protein; Brn3A-Brain-specific homeobox/POU domain protein 3A; GAPDH-Glyceraldehyde 3-phosphate dehydrogenase. Densitometric analyses are shown in the lower panel. N = 3–4 mice from each group. *P < 0.05 as compared with WT and #P < 0.05 as compared with AIF deficient mice.

2.6. Western blot analyses

Denatured proteins from either mouse retinal samples or 661 W cells were separated by SDS- polyacrylamide gels (4–12% Tricine gels) and electroblotted onto PVDF membranes. The membranes were blocked with 5% non-fat dry milk in TBS with 0.1% Tween 20, incubated overnight with primary antibodies (dilution 1:1000), probed with near-Infrared Fluorescent Secondary Antibodies (LI-COR) (dilution 1:10000), and visualized with an Odyssey imaging system (LI-COR). The band intensities were quantified, and protein expression levels were calculated relative to either actin or GAPDH from the same membrane after stripping.

2.6.1. NADH and NAD quantitation

NAD^+ and NADH were extracted and quantified from cell lysates using a specific kit (Abcam, ab65348) following the manufacturer's instructions that exclude interaction with NADP and NADPH.

2.7. Separation of mitochondria rich-fraction from retina

We used a procedure adapted from that for adrenal cortical mitochondria separation [41] to isolate mitochondria rich-fraction from retinal tissue [42]. Briefly, each individual experiment used three pairs of mice retinas from the same experimental group. Retinas were suspended in ice-cold MSM-EDTA medium (220 mM mannitol, 70 mM sucrose, 10 mM MOPS, 2 mM EDTA, pH 7.4), and hand homogenized in Eppendorf tubes. The homogenate was centrifuged at 800 g for 10 min, and the remaining supernatant was centrifuged at 14,000 for 10 min. The resultant pellet was washed twice in the isolation buffer. The final pellet was re-suspended in isolation buffer.

2.8. Activities of mitochondrial electron chain complexes (ETC) complexes

ETC complex activities were measured as specific donor-acceptor oxidoreductase activities as described [43,44]. Briefly, NADH dehydrogenase of complex I was measured as the consumption of NADH at 340 nm in the presence of ferricyanide as an electron acceptor. The NADH-cytochrome c oxidoreductase was assessed as the rotenone-sensitive reduction of oxidized cytochrome c at 550 nm.

2.9. Cell survival

Photoreceptor-like 661 W cells were seeded at 10,000 cells per well in a 96-well plate, grown to 80% confluence, and incubated with various concentrations of rotenone (0–20 μM) and methylene blue (0-30μM) for 24 h. Following treatment, cell survival was assessed through an MTT assay according to the manufacturer's protocol.

ATP level was determined in 661 W cells incubated with rotenone and MB using a Luminescent ATP Detection Assay kit (ab113849) according to the manufacture's instructions.

Mitochondrial reactive oxygen species (ROS) generation was measured with MitoSox red superoxide indicator as described [45].

Mitochondrial membrane potential was measured on cells grown to 80% confluence on 96-well plates with JC-1, a cationic dye that exhibits potential-dependent mitochondrial accumulation, according to the manufacturer's instruction. Briefly, we recorded the fluorescence emission at red (590 nm) and green (525 nm) indicating the concentration-dependent formation and dissipation, respectively, of red fluorescent J aggregates within the mitochondria. The shift from red to green fluorescence indicates mitochondrial depolarization.

2.9.1. Statistical analysis

Data were evaluated for statistical differences amongst groups using student's 2 tailed-*t*-test and a two-way ANOVA followed by Bonferroni's multiple comparison test. Data are reported as mean ± SEM with data representing n = 3–7 per group. Significance was established at $\#p < 0.05$

3. Results

3.1. AIF deficiency causes retinal thinning that is alleviated by methylene blue (MB) treatment

AIF deficiency causes a significant decrease in the retinal thickness that is observed in all retinal layers. The administration of MB inhibited the decrease in retinal thickness in the Hq mice (Fig. 1**A**). Confocal microscopy of the DAPI-stained retinal sections similarly show the rarefaction of nuclei in all retinal layers, which was prevented by the MB treatment (Fig. 1**B**). We further performed western blot analysis of retinal layer marker proteins in order to delineate the effect of AIF-deficiency and MB therapy. We confirmed that mitochondrial complex I defect causes damage of the inner retinal ganglion cells [15] as the retinal ganglion cell marker, Brn3A, was significantly decreased by the AIF deficiency; its expression was preserved by the MB treatment (Fig. 1**C**). The expression level of glial fibrillary acidic protein (GFAP), normally present in retinal astrocytes, Muller cells and optic nerve oligodendrocytes, also was mildly decreased by AIF deficiency suggesting a rarefaction of those retinal cells, and was improved by the MB treatment.

3.2. AIF deficiency damages the retinal photoreceptors that were preserved by the MB treatment

Due to the observed damaging effect of the AIF deficiency on all retinal layers including the outer nuclear retinal layer and the protective effect of MB treatment, we further focused our study on photoreceptors, which are the retinal cells supporting this nuclear layer. Photoreceptors are light sensitive neurons, and occur as cones and rods, with the latter being predominant in mice. The most specific features of photoreceptors are their outer segments, which are cylindrical structures containing stacks of membranous discs filled with light-sensitive proteins called opsin and rhodopsin, respectively. We assessed the integrity of photoreceptors by electron microscopy, confocal microscopy and western blot analysis.

Electron microscopy was used to evaluate the ultrastructure of the photoreceptor outer segments (Fig. 2**A**). In wild-type mice, the outer segments appear as straight parallel cylinders comprising long arrays of stacked membranous discs oriented perpendicular to the long axis. Retinal pigment epithelial cells send slender membranous processes extending to the adjacent photoreceptor cells. Photoreceptor outer segments were abnormal in the AIF deficient mice. While the discs maintained their perpendicular orientation and diameters, their numbers were significantly decreased. The nascent discs were still aligned along the axoneme at the base of the outer segment suggesting that AIF deficiency did not alter the formation of the outer segments, and that the shortening of the outer segments is not induced by a defect in the initiation of morphogenesis. The integrity and thickness of the retinal outer segments were completely preserved by the MB treatment (Fig. 2**A**).

The observed decrease in photoreceptor outer membranous discs was confirmed by confocal microscopy (Fig. 2**B**) that showed a dramatic decrease in the expression of the light-sensitive marker pigment, rhodopsin, in mice with AIF deficiency. This method also showed the protective effect of the MB treatment. Western blot analyses confirmed the decrease in the expression of both rhodopsin (marker of rod photoreceptors) and red/green opsin (marker of cone photoreceptors) amounts in the AIF-deficient retinas, and that these levels of expression were preserved by the MB treatment (Fig. 2**C**).

3.3. MB treatment preserves mitochondrial density in the retinal photoreceptors by preserving mitochondrial integrity and decreasing mitophagy

Mitochondria are packed in the inner segments of photoreceptor cells, just underneath the outer segments. Mitochondrial density in the whole retina was determined by assessing the expression levels of mitochondrial marker proteins (Fig. 3**A**). We found that the complex I subunit NDUFB8, cytochrome c and citrate synthase were decreased in the AIF-deficient retinas, and their expression was improved by MB, consistent with MB treatment preventing the decrease in mitochondrial density induced by AIF deficiency.

We questioned if this change in retinal mitochondrial density is induced either by alterations in mitochondrial formation via biogenesis pathway or by elimination via mitophagy. Mitochondrial biogenesis signal was not changed by either AIF deficiency or MB treatment as shown by the unaffected expression of the master regulator of this process, PGC1α (Fig. 3**B**). In contrast, we observed that AIF deficiency increased the number of mitochondria with damaged/absent cristae in the inner segments of photoreceptor cells (Fig. 3**C**). We also observed double membrane-autophagic vesicles in the photoreceptor layers of AIF-deficient retinas. Mitochondrial structure and cristae integrity was preserved by MB treatment (Fig. 3**C**).

We then questioned if the observed increased mitochondrial damage leads to enhanced mitochondrial elimination by mitochondrial-induced autophagy (mitophagy flux). Markers of autophagy (LC3B-II and beclin I) were increased by AIF deficiency. PINK1 protein level was also increased by AIF deficiency indicating a decreased degradation of PINK1 by damaged or depolarized mitochondria. MB treatment corrected these abnormalities indicating a normalization of the mitophagic flux (Fig. 3**D**).

3.4. MB normalizes complex I activity in the AIF-deficient retina

In order to understand if MB prevents retinal damage by improving the electron flow within the mitochondrial electron transport chain, we assessed the NADH oxidation (electron input) and cytochrome c reduction (electron output) by retinal mitochondrial-rich fraction (Fig. 4). NADH consumption was measured spectrophotometrically at 340 nm in the presence of the electron acceptor, ferricyanide (NADH ferricyanide reductase, NFR). AIF deficient mitochondria had a lower ability to oxidize NADH, a deficiency that was corrected by the addition of 30 μM MB to the mitochondrial suspension, indicating that MB as an electron

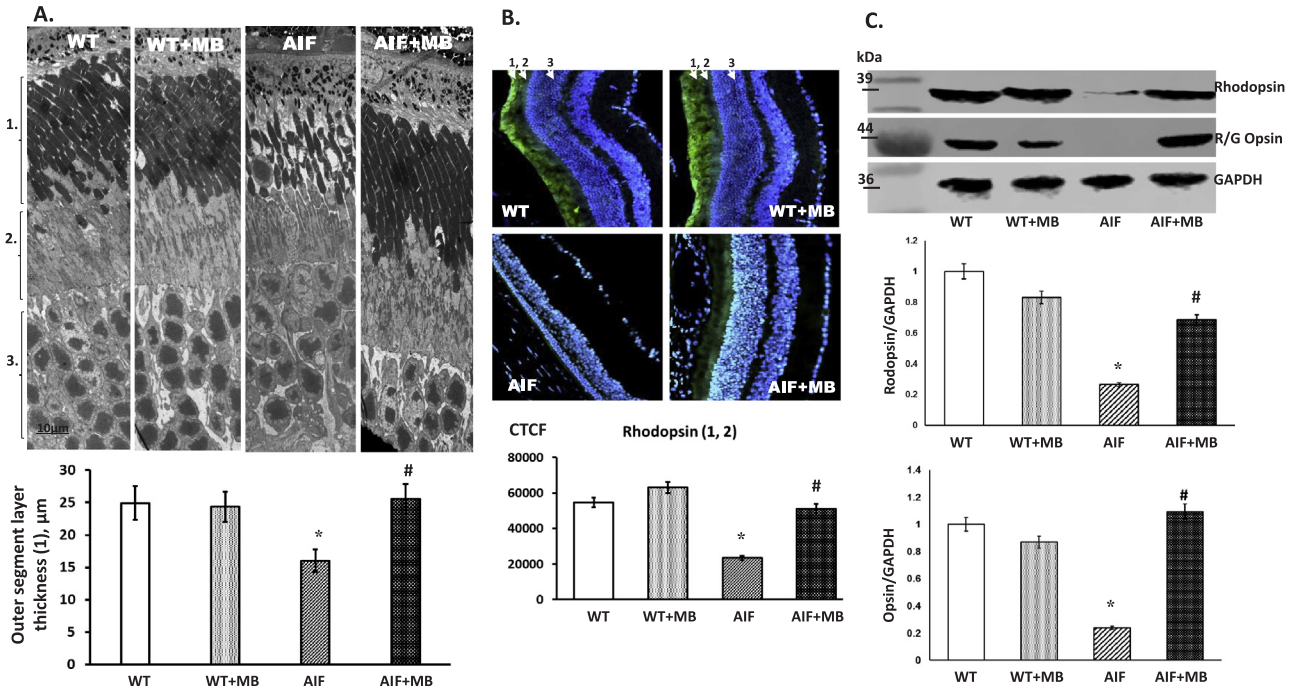

Fig. 2. MB treatment preserves the retinal photoreceptor cells and their outer segments that were damaged by AIF deficiency. A. Electron microscopic images of the outer retinas from wild type mice (WT), wild type mice treated with methylene blue (WT + MB), AIF deficient mice (AIF), and AIF-deficient mice treated with methylene blue (AIF + MB). The numbers represent the outer retina layers: 1-outer segments, 2-inner segments, 3-outer nuclear layer. The thickness of the outer segment layer [1] is presented in the lower panel. **B.** Confocal images depicting the green fluorescent rhodopsin distribution in the retinal outer layers of wild type mice (WT), wild type mice treated with methylene blue (WT + MB), AIF deficient mice (AIF), and AIF-deficient mice treated with methylene blue (AIF + MB). The amount of rhodopsin in the outer [1] and inner [2] segment layers is presented in the lower panel as corrected total cellular fluorescence (CTCF). **C.** Western blot analyses for rhodopsin (marker of rod photoreceptor cells) and red/green opsin (R/G opsin, marker of cone photoreceptor cells). GAPDH-Glyceraldehyde 3-phosphate dehydrogenase. Densitometric analyses are shown in the lower panel. N = 3–4 mice from each group were used for statistical analyses. *P < 0.05 as compared with WT and #P < 0.05 as compared with AIF deficient mice.

acceptor complements complex I in oxidizing NADH.

The reduction of exogenously added oxidized cytochrome c was measured spectrophotometrically at 550 nm in the presence of NADH as electron donor and cytochrome c as electron acceptor (NADH-cytochrome c oxidoreductase, NCR). The reaction measures the activities of complex I and III linked by coenzyme Q. Because rotenone limits the conventional complex I-to-complex III electron transport by inhibiting the complex I-Q binding site, the rotenone-sensitive rates show the specific CI-III activities. As expected, the ability of AIF-deficient mitochondria to transfer electrons from NADH to cytochrome c is decreased. This function is rotenone-sensitive (Rs) indicating that the limit is at the level of complex I. The rotenone-sensitive NADH-cytochrome c electron transport was improved by MB, indicating that MB mediates the transfer of electron from NADH to cytochrome c through complex I. MB is also able to increase the rotenone-insensitive NADH-cytochrome c oxidoreductase rates (Ri); the insensitivity to rotenone (Ri) indicates that MB also provides an alternative pathway for electron transfer (in addition to the canonical electron transfer through complex I).

3.5. MB protects the integrity of complex I defective 661W cells, improves mitochondrial metabolism and redox state, and inactivates the mitochondrial stress pathways UPR^{mt} and mitophagy

The negative impact of complex I deficiency on photoreceptor cell survival observed in vivo may be mediated by either a drop in mitochondrial membrane potential and ATP generation, an increase in the NADH/NAD$^+$ redox ratio or an increase in oxidative stress. In order to unfold the mechanisms of MB protective effect we used an in vitro photoreceptor-like cell system, the 661W cells. Complex I defect was induced by treating the 661W cells with rotenone. We found that rotenone decreases cell survival in a dose-dependent manner (Fig. 5**A**). Methylene blue (30 μM) added during the rotenone incubation normalized the cell survival rates.

We further focused on the impact of mitochondrial complex I defect on bioenergetics in photoreceptor-like cells, and the effect of MB. We found that the rotenone-induced complex I defect caused a decrease in ATP generation, which was not prevented by MB at concentrations that were observed to promote cells survival (Fig. 5**B**). In contrast, MB treatment prevented mitochondrial depolarization (Fig. 5**C**) and the increase in ROS generation (Fig. 5**D**), and normalized the NADH/NAD$^+$ ratio (Fig. 5**E**). These effects were achieved by lower (15 μM) MB concentrations compared to those necessary to prevent cell death (30 μM), indicating that the MB-induced decrease in oxidative and redox stress rather than preventing energy deprivation were upstream phenomena that promoted the photoreceptor-like cell survival.

We further explored if a defect in mitochondrial complex I triggered a mitochondrial stress response pathways by examining mitochondrial-induced autophagy and the unfolded protein response (UPR^{mt}) (Fig. 6). We found that the lipidated form of the microtubule-associated protein 1 light chain 3B (LC3B-II), a hallmark of autophagy, was increased in rotenone-treated photoreceptor-like cells. Beclin 1, the mammalian orthologue of yeast Atg6 with a central role in autophagy, had similar changes. The activation of the mitochondrial unfolded protein response (UPR^{mt}), a mitochondrial-specific response to proteotoxic stress, was investigated by assessing the level of the mitochondrial chaperone and quality control protein, heat shock protein 60 (HSP60). The rotenone-induced complex I defects caused an increased HSP60 level. Mitochondrial stress response pathways were normalized by the addition of MB.

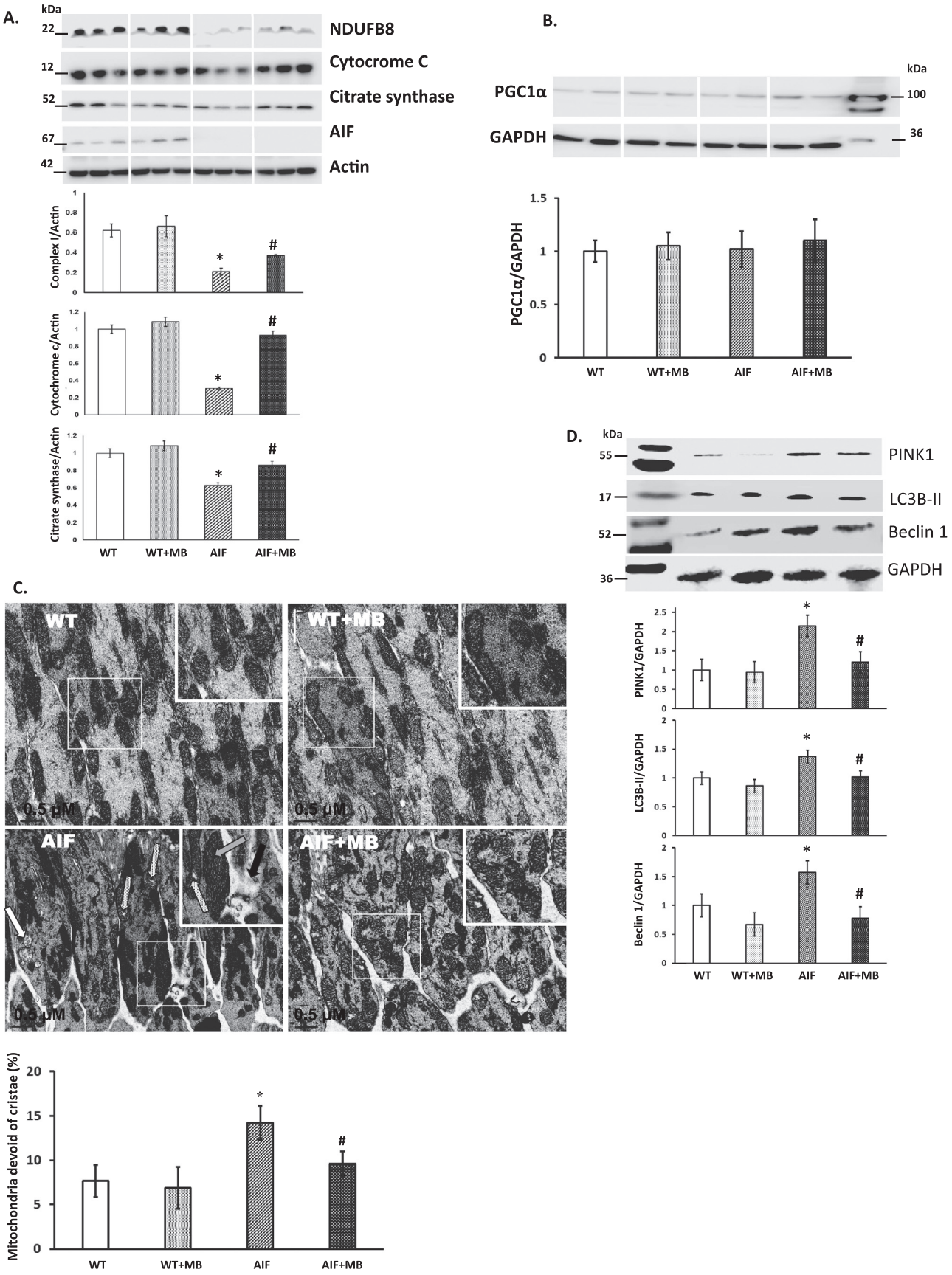

(caption on next page)

Fig. 3. MB preserves mitochondrial density in the retinal photoreceptors by preserving mitochondrial integrity and decreasing mitophagy. A. Western blot analyses of mitochondrial marker proteins. Densitometric analyses are shown in the lower panel. B. Western blot analyses of the master regulator of mitochondrial biogenesis, the peroxisome proliferator activated receptor γ c-activator α (PGC1α). Densitometric analyses are shown in the lower panel. C. Electron microscopic images of the inner segments of retinas from wild type mice (WT), wild type mice treated with methylene blue (WT + MB), AIF deficient mice (AIF), and AIF-deficient mice treated with methylene blue (AIF + MB). The black arrow shows an area in a photoreceptor cell that is damaged and devoid of mitochondria. The gray arrow shows a mega-mitochondria, while the dotted arrow shows mitochondria devoid of cristae. Double-membrane autophagic vesicles are indicated by white arrow. Damaged mitochondria (mitochondria with areas devoid of cristae) were counted on EM photographs, and expressed per 100 counted mitochondria. D. Western blot analyses of mitochondrial-induced autophagy markers. PINK1-PTEN-induced putative kinase 1, LC3B-II-Light Chain 3B-II, GAPDH-Glyceraldehyde 3-phosphate dehydrogenase. Densitometric analyses are shown in the lower panel. N = 3–4 mice from each group were used for statistical analyses. *P < 0.05 as compared with WT and #P < 0.05 as compared with AIF deficient mice.

4. Discussion

Diseases of the inner retina, in particular death and rarefaction of the ganglion layer neurons leading to optic nerve atrophy and blindness, have been reported as clinical features of mitochondrial complex I defect [5]. AIF deficiency in Harlequin mice also affects the inner retina [9]. However, the largest number of mitochondria is located in the outer retina, which includes retinal photoreceptor and pigmental cells. Retinal photoreceptors, the light-sensitive neurons critical for vision, have the highest density of mitochondria packed in their inner segments [7,8], highest immunoreactivity for OXPHOS enzymes [46], rates of OXPHOS [47], energy demand and dependence on OXPHOS (90–95%) for ATP generation [48,49], and are responsible for retinal oxidative damage in chronic diabetic conditions [37]. In contrast with the inner retinal neurons, mouse photoreceptors perform at their maximal respiratory capacity in basal conditions with a very limited reserve [50], suggesting that small reductions in OXPHOS could have a severe impact on their survival. Mitochondrial-induced cellular damage is associated with a large number of photoreceptor dystrophies [6]. Despite these data, the effect of OXPHOS defects on photoreceptor integrity and bioenergetics has not been studied. Our study revealed that retinal photoreceptor cells are sensitive to a mitochondrial complex I defect.

While the highest density of mitochondria is packed in the inner segments of photoreceptors, the outer segments have also been reported to express electron transfer chain complexes, and conduct oxidative ATP production necessary for the phototransduction cascade [51]. Photoreceptor outer segments are specialized sensory cilia with hundreds of membrane discs containing photo-transduction proteins, and are renewed by opposing processes of disk morphogenesis and shedding. Disk renewal requires protein and lipid synthesis in the inner segment of photoreceptors, a substructure located beneath the outer segment. Approximately 10% of the rod photoreceptor outer segment is daily engulfed in phagosomes of the retinal pigment cells, and the protein and lipid cargo degraded [52]. The synthesis and polarized transport of lipids and proteins is energetically demanding [53]. Rhodopsin, a seven-transmembrane helix receptor superfamily [54], represents 90% of total protein content in the rod outer segments, and serves both functional and structural roles as rhodopsin knockout mice are unable to elaborate outer segments [55]. While other retinal layers

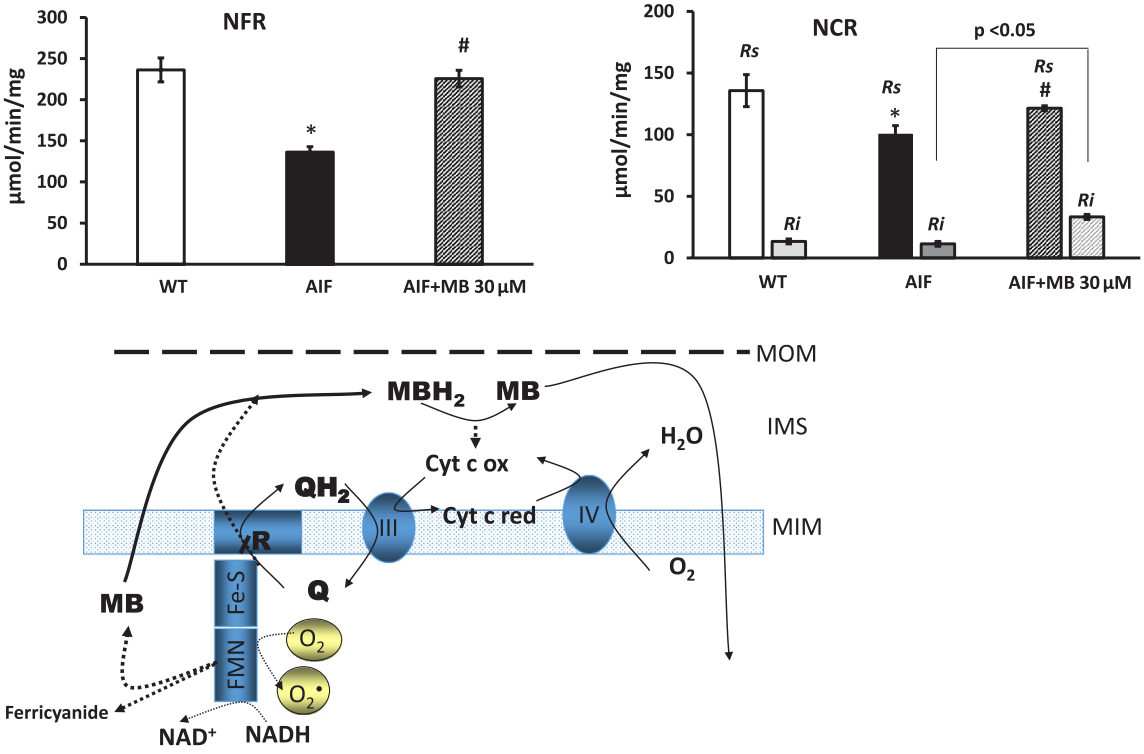

Fig. 4. MB improves complex I activity in the AIF-deficient retina. NADH dehydrogenase was measured as the consumption of NADH at 340 nm in the presence of ferricyanide as an electron acceptor (NADH ferricyanide reductase, NFR). The NADH-cytochrome c oxidoreductase (NCR) was assessed as the rotenone-sensitive reduction of oxidized cytochrome c at 550 nm. The assays were performed in mitochondrial enriched fractions from wild type (WT) and AIF-deficient (AIF) retinas. The results are expressed in µmol/min/mg mitochondrial protein. Methylene blue (MB, 30 µM) was added in the reaction mixture. The lower panel shows a proposed redox cycle for MB in retinal mitochondria. N = 3 retinas from each group were used for statistical analyses. *P < 0.05 as compared with WT and #P < 0.05 as compared with AIF deficient mice. MOM = mitochondrial outer membrane, IMS = intermembrane space, MIM = mitochondrial inner membrane, R = Rotenone, Cyt c = Cytochrome c, Ox = Oxidized, Red = Reduced.

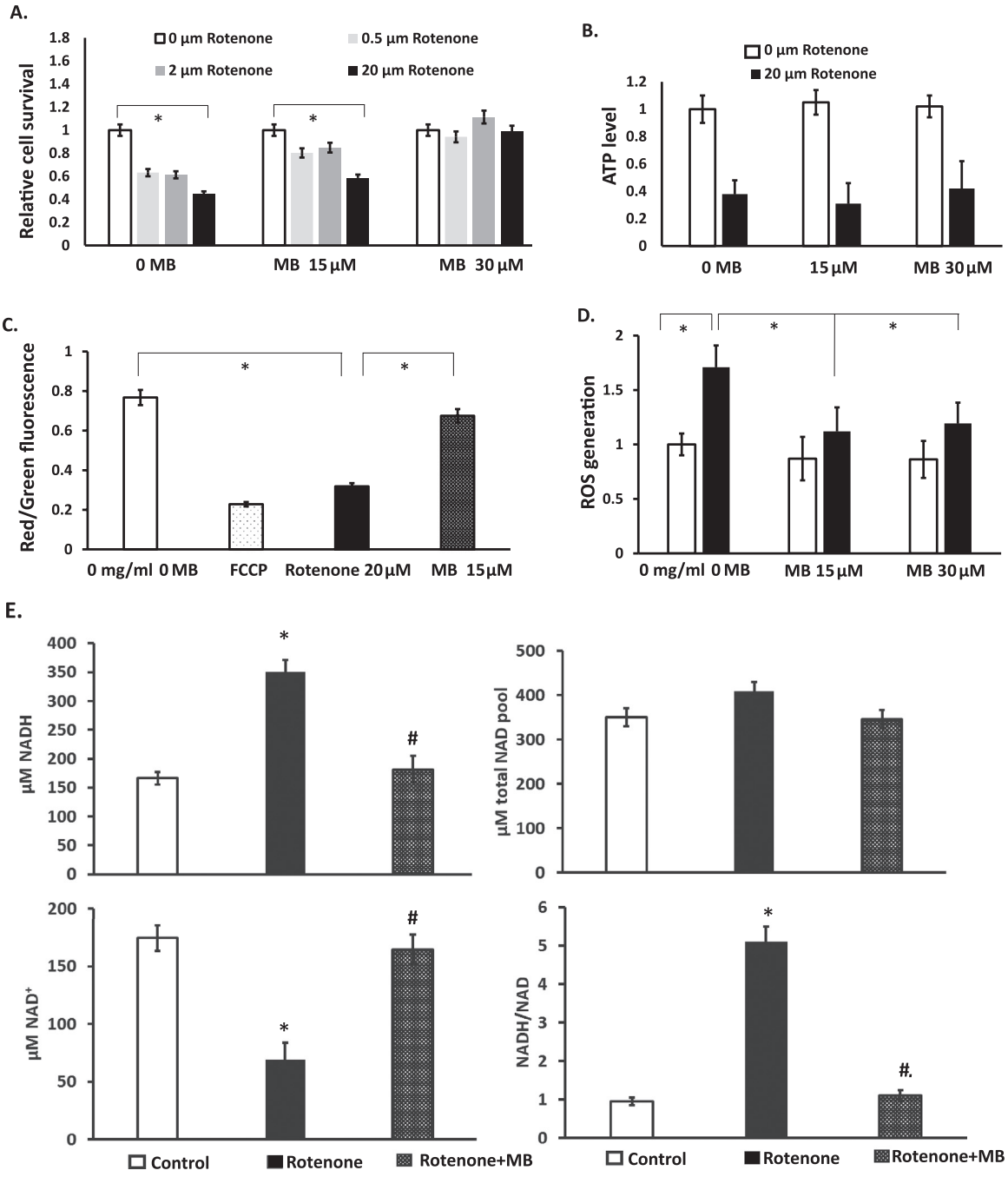

Fig. 5. MB protects the integrity of complex I defective 661 W cells and improves mitochondrial metabolism and redox state. A. Photoreceptor-like 661 W cells were grown to 80% confluence under the conditions described, and treated for 24 h with Rotenone with/without methylene blue (MB). Cell survival during these experimental conditions is expressed as a ratio compared to cells maintained in basal conditions. **B.** ATP level was measured by a colorimetric assay, and the results expressed as a ratio compared to cells maintained in basal conditions. **C.** Mitochondrial membrane potential is expressed as the Red/Green/fluorescence of the cationic JC1 compound. **D**. Mitochondrial ROS generation was measured as superoxide, and the results expressed as a ratio compared to cells maintained in basal conditions. **E.** The reduced (NADH) and oxidized (NAD^+) forms of NAD were extracted and quantified as described. The data are the results of two independent experiments. *P $<$ 0.05 as compared with control and #P $<$ 0.05 as compared with rotenone treated photoreceptor cells.

are also affected, the effect of mitochondrial complex I defect on decreasing the photoreceptors and their outer segments is significant. We show that the nascent discs still maintained their alignment along the axoneme, perpendicular orientation and diameters suggesting that AIF-deficient photoreceptor cells retained an intact ability to build outer segments, and that the decrease in discs number is not induced by a defect in morphogenesis. Both the number of discs and their protein markers were corrected to normal levels by improving the complex I-induced disruption in the mitochondrial electron flow with a redox compound, methylene blue (MB). Our results stress the importance of mitochondrial integrity in maintaining the photoreceptors and their outer segment discs.

Electrons derived from NADH are normally accepted by FMN during NADH oxidation by mitochondrial complex I. Methylene blue (MB) is a substrate for NADH dehydrogenase, which reduces MB to MBH2, the latter donating electrons further to cytochrome c [56]. Therefore, the alternative electron transport provided by MB bypasses defects in either complexes I or III. We observed that MB facilitates NADH oxidation

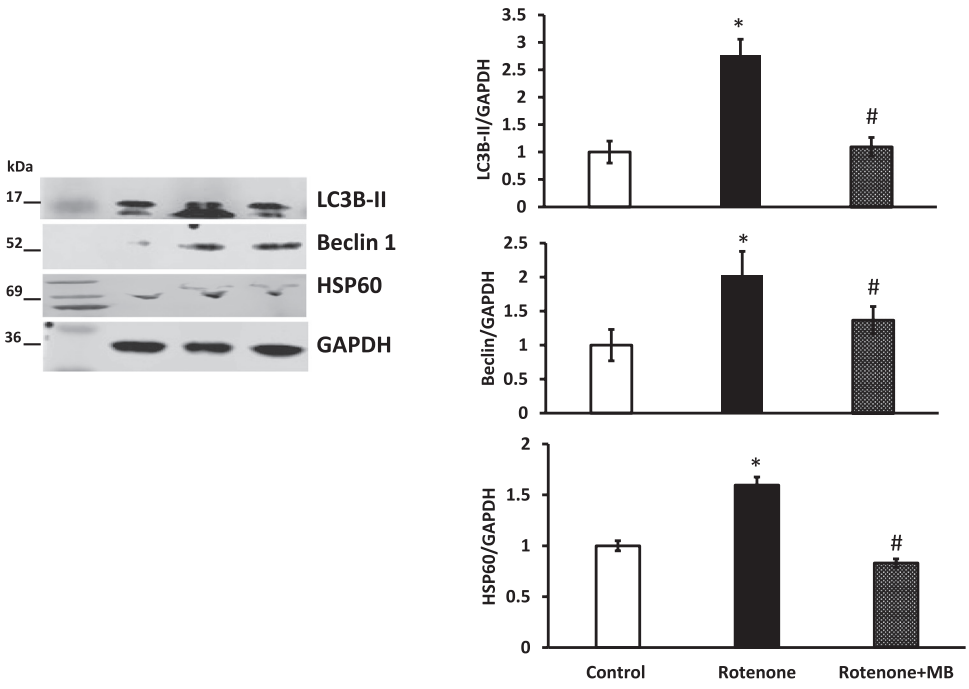

Fig. 6. MB treatment deactivates mitochondrial stress pathways, UPR^{mt} and mitophagy, in the complex I deficient 661 W photoreceptor like cells. Western blot analyses of mitochondrial-induced autophagy markers. LC3B-II: Light Chain 3B, HSP60: Heat Shock Protein 60, GAPDH: Glyceraldehyde 3-phosphate dehydrogenase. Densitometric analyses are shown in the right panel. The data are the results of at least two independent experiments. *P < 0.05 as compared with control and #P < 0.05 as compared with rotenone treated photoreceptor cells.

while recovering NAD^+ in photoreceptor-like cells (Fig. 4) and energized cardiac mitochondria [57]. Therefore, electrons derived from NADH may be shared between an alternative redox loop supported by MB and the classical in-chain pathway via FMN through a linear series of Fe-S centers to the acceptor, ubiquinone. As NADH does not donate electrons directly to MB, the redox potential would allow either FMN or Fe-S center to be the electron donors to MB that has a low redox potential of 11 mV. In order to identify the electron donor to MB we added an additional electron acceptor, ferricyanide, which is a direct electron acceptor from FMN. The increase in NADH oxidation indicates that FMN rather than the Fe-S centers is the electron donor to MB. An interesting finding was that MB facilitates both the rotenone insensitive and sensitive NADH cytochrome c reductase in retinal mitochondria. The increase in cytochrome c reduction by MB confirms that the electron acceptor is cytochrome c. As rotenone inhibits complex I at the Q-binding site, the improvement of rotenone-sensitive cytochrome c reduction upon MB addition indicates that Q binding site is part of the MB redox loop.

Mitochondrial alterations trigger a quality control system represented by the unfolded protein response (UPR^{mt}) and mitophagy. Misfolded/unfolded proteins and failed-imported proteins are degraded by the mitochondrial proteolytic system. As a response to mitochondrial damage, the mitochondrial phosphatase and tensin homolog (PTEN)-induced kinase 1 (PINK1) is stabilized on the outer mitochondrial membrane, and recruits the cytosolic E3 ubiquitin ligase Parkin that initiates mitophagy [58]. PINK1 functions as a mitochondrial stress sensor [59,60]. The LC3 protein is a ubiquitin-like protein that is conjugated to phosphatidylethanolamine being converted to LC3-II that is a marker for mitophagy. Complex I defect may create a mitochondrial protein misfolding environment and activate multiple mitochondrial stress responses. For example, increased oxidative stress causes protein oxidative modifications leading to protein misfolding, thus potentially activating UPR^{mt}. The decrease in mitochondrial membrane potential triggers PINK1-mediated mitophagy [58]. A pharmacological inhibition of complex I led to mitochondrial transition pore opening and depolarization, increased mitochondrial oxidative stress, and triggered mitophagy and cell death [61] while increasing oxidative stress activated both UPR^{mt} and mitophagy [62]. In agreement with this concept, we found that complex I defect activates both UPR^{mt} and mitophagy in retina and photoreceptor-like cells, and that both mitochondrial stress response pathways were inhibited by MB.

From all retinal cells, photoreceptors are the most susceptible to depletion of the total cellular NAD pool [63]. In comparison with the cytosolic and nuclear NAD pool, the mitochondrial NAD pool is finely-balanced and relatively high matching the critical role of NAD in mitochondrial function [64]. The decrease in cellular total NAD pool severely compromises primarily mitochondrial metabolism particularly NAD^+-dependent TCA enzymes and mitochondrial lysine deacetylases, sirtuins, causing photoreceptor death [63]. The reduction in the total cellular NAD pool also blunts the adaptive UPR^{mt} pathway [65], leading to proteotoxic stress, and accumulation of damaged depolarized mitochondria [66]. NAD occurs as either oxidized (NAH^+) or reduced (NADH) forms. While NADH is the result of substrate oxidation the NAD^+ is an important cofactor for mitochondrial enzymes. Therefore, the NADH/NAD^+ ratio reflects the overall status of mitochondrial metabolism. While the amount of NADH production and NAD^+ consumption are tightly linked to fuel oxidation, mitochondrial NAD recycling (NADH consumption and NAD^+ production) is decreased by ETC defects. For example, complex I defect causes an increased mitochondrial NADH content causing a highly-reduced redox environment within mitochondria, and decreases the available NAD^+ [67]. An approach to correcting mitochondrial ETC defects is increasing NAD^+ content [68].

In human skin fibroblasts, a decrease in complex I activity is positively correlated with increased oxidative stress and altered mitochondrial morphology [69]. We have confirmed these results, and showed that MB treatment corrected these abnormalities. Unexpectedly, a cardiac complex I defect did not result in basal ATP depletion or increased ROS production [67] but rather increased the mitochondrial NADH/NAD^+ redox ratio and opening probability of the mitochondrial permeability pore [67] with an increased risk of cardiomyocyte apoptosis. Similar to cardiac mitochondria, we found that complex I deficient retinal mitochondria do not exhibit an energy deficit but showed a similar NAD^+ deficit, increased NADH/ NAD^+ redox ratio and mitochondrial depolarization. In contrast with cardiac complex I defect, the decrease in complex I activity in the retina leads to increased oxidative stress suggesting that the interruption of electron flow in complex I favors reactive oxygen species generation. In agreement to our findings, the Leber hereditary optic neuropathy mouse model revealed that optic nerve atrophy is induced by the complex I

deficiency induced-oxidative stress rather than energy deficit [5]. The univalent reduction of oxygen to form superoxide occurs with increased electron pressure at specific ETC sites caused by interruption of the electron flow in ETC defects thus creating a mitochondrial reductive redox stress. Due to its redox potential MB cannot accept electrons directly from superoxide and be a canonical superoxide scavenger. An alternative and plausible explanation is that MB relieves the reductive redox stress by complementing complex I in oxidizing NADH and regenerating NAD^+.

5. Conclusion

We report that preserving the mitochondrial integrity is critical for the maintenance of the photoreceptors and their outer segments. MB or other compounds with similar mechanism of action may be therapeutic options for the retinal disease induced by mitochondrial complex I deficiency.

Acknowledgments

We acknowledge Dr. Al-Ubaidi Muayyad (University of Huston) for the generous gift of 661W photoreceptor-like cells. We thank Haitao Liu and Dr. Timothy Kern's laboratory (Case Western Reserve University, Cleveland, Ohio) for histologic measurements of the retina and helpful suggestions, and Dr. Hisashi Fujioka (Electron Microscopy Core Facility, Case Western Reserve University) for the electron microscopy work. We appreciate the invaluable input of Dr. Edward McKee (Central Michigan University College of Medicine), and the technical and editorial help of Carmen Avramut (Medical student, Central Michigan University, College of Medicine) and Joel Santos (undergraduate, Central Michigan University).

Funding

This work was provided by a research award from the United Mitochondrial Disease Foundation (12-97, to MR), and NIH grants EY022938 and R24 EY024864, and a Merit grant from the Department of Veteran Affairs (to Dr. Timothy Kern).

References

[1] P. Benit, S. Goncalves, E.P. Dassa, J.J. Briere, P. Rustin, The variability of the harlequin mouse phenotype resembles that of human mitochondrial-complex I-deficiency syndromes, PloS One 3 (2008) e3208.
[2] S. DiMauro, E.A. Schon, Mitochondrial respiratory-chain diseases, New Engl. J. Med. 348 (2003) 2656–2668.
[3] A.A. Sadun, C. La Morgia, V. Carelli, Leber's hereditary optic neuropathy, Curr. Treat. Options Neurol. 13 (2011) 109–117.
[4] D.C. Wallace, G. Singh, M.T. Lott, J.A. Hodge, T.G. Schurr, A.M. Lezza, L.J. Elsas 2nd, E.K. Nikoskelainen, Mitochondrial DNA mutation associated with Leber's hereditary optic neuropathy, Science 242 (1988) 1427–1430.
[5] C.S. Lin, M.S. Sharpley, W. Fan, K.G. Waymire, A.A. Sadun, V. Carelli, F.N. Ross-Cisneros, P. Baciu, E. Sung, M.J. McManus, B.X. Pan, D.W. Gil, G.R. Macgregor, D.C. Wallace, Mouse mtDNA mutant model of Leber hereditary optic neuropathy, Proc. Natl. Acad. Sci. USA 109 (2012) 20065–20070.
[6] E. Lefevere, A.K. Toft-Kehler, R. Vohra, M. Kolko, L. Moons, I. Van Hove, Mitochondrial dysfunction underlying outer retinal diseases, Mitochondrion 36 (2017) 66–76.
[7] Q.V. Hoang, R.A. Linsenmeier, C.K. Chung, C.A. Curcio, Photoreceptor inner segments in monkey and human retina: mitochondrial density, optics, and regional variation, Vis. Neurosci. 19 (2002) 395–407.
[8] J. Stone, D. van Driel, K. Valter, S. Rees, J. Provis, The locations of mitochondria in mammalian photoreceptors: relation to retinal vasculature, Brain Res. 1189 (2008) 58–69.
[9] J.A. Klein, C.M. Longo-Guess, M.P. Rossmann, K.L. Seburn, R.E. Hurd, W.N. Frankel, R.T. Bronson, S.L. Ackerman, The harlequin mouse mutation downregulates apoptosis-inducing factor, Nature 419 (2002) 367–374.
[10] S.A. Susin, H.K. Lorenzo, N. Zamzami, I. Marzo, B.E. Snow, G.M. Brothers, J. Mangion, E. Jacotot, P. Costantini, M. Loeffler, N. Larochette, D.R. Goodlett, R. Aebersold, D.P. Siderovski, J.M. Penninger, G. Kroemer, Molecular characterization of mitochondrial apoptosis-inducing factor, Nature 397 (1999) 441–446.
[11] D. Arnoult, P. Parone, J.C. Martinou, B. Antonsson, J. Estaquier, J.C. Ameisen, Mitochondrial release of apoptosis-inducing factor occurs downstream of cytochrome c release in response to several proapoptotic stimuli, J. Cell Biol. 159 (2002) 923–929.
[12] M.D. Miramar, P. Costantini, L. Ravagnan, L.M. Saraiva, D. Haouzi, G. Brothers, J.M. Penninger, M.L. Peleato, G. Kroemer, S.A. Susin, NADH oxidase activity of mitochondrial apoptosis-inducing factor, J. Biol. Chem. 276 (2001) 16391–16398.
[13] M.J. Mate, M. Ortiz-Lombardia, B. Boitel, A. Haouz, D. Tello, S.A. Susin, J. Penninger, G. Kroemer, P.M. Alzari, The crystal structure of the mouse apoptosis-inducing factor AIF, Nat. Struct. Biol. 9 (2002) 442–446.
[14] H. Ye, C. Cande, N.C. Stephanou, S. Jiang, S. Gurbuxani, N. Larochette, E. Daugas, C. Garrido, G. Kroemer, H. Wu, DNA binding is required for the apoptogenic action of apoptosis inducing factor, Nat. Struct. Biol. 9 (2002) 680–684.
[15] N. Vahsen, C. Cande, J.J. Briere, P. Benit, N. Joza, N. Larochette, P.G. Mastroberardino, M.O. Pequignot, N. Casares, V. Lazar, O. Feraud, N. Debili, S. Wissing, S. Engelhardt, F. Madeo, M. Piacentini, J.M. Penninger, H. Schagger, P. Rustin, G. Kroemer, AIF deficiency compromises oxidative phosphorylation, EMBO J. 23 (2004) 4679–4689.
[16] E. Hangen, O. Feraud, S. Lachkar, H. Mou, N. Doti, G.M. Fimia, N.V. Lam, C. Zhu, I. Godin, K. Muller, A. Chatzi, E. Nuebel, F. Ciccosanti, S. Flamant, P. Benit, J.L. Perfettini, A. Sauvat, A. Bennaceur-Griscelli, K. Ser-Le Roux, P. Gonin, K. Tokatlidis, P. Rustin, M. Piacentini, M. Ruvo, K. Blomgren, G. Kroemer, N. Modjtahedi, Interaction between AIF and CHCHD4 regulates respiratory chain biogenesis, Mol. Cell 58 (2015) 1001–1014.
[17] E. Hangen, K. Blomgren, P. Benit, G. Kroemer, N. Modjtahedi, Life with or without AIF, Trends Biochem Sci. 35 (2010) 278–287.
[18] E. Hangen, D. De Zio, M. Bordi, C. Zhu, P. Dessen, F. Caffin, S. Lachkar, J.L. Perfettini, V. Lazar, J. Benard, G.M. Fimia, M. Piacentini, F. Harper, G. Pierron, J.M. Vicencio, P. Benit, A. de Andrade, G. Hoglinger, C. Culmsee, P. Rustin, K. Blomgren, F. Cecconi, G. Kroemer, N. Modjtahedi, A brain-specific isoform of mitochondrial apoptosis-inducing factor: AIF2, Cell Death Differ. 17 (2010) 1155–1166.
[19] J.A. Pospisilik, C. Knauf, N. Joza, P. Benit, M. Orthofer, P.D. Cani, I. Ebersberger, T. Nakashima, R. Sarao, G. Neely, H. Esterbauer, A. Kozlov, C.R. Kahn, G. Kroemer, P. Rustin, R. Burcelin, J.M. Penninger, Targeted deletion of AIF decreases mitochondrial oxidative phosphorylation and protects from obesity and diabetes, Cell 131 (2007) 476–491.
[20] I. Berger, Z. Ben-Neriah, T. Dor-Wolman, A. Shaag, A. Saada, S. Zenvirt, A. Raas-Rothschild, M. Nadjari, K.H. Kaestner, O. Elpeleg, Early prenatal ventriculomegaly due to an AIFM1 mutation identified by linkage analysis and whole exome sequencing, Mol. Genet. Metab. 104 (2011) 517–520.
[21] D. Ghezzi, I. Sevrioukova, F. Invernizzi, C. Lamperti, M. Mora, P. D'Adamo, F. Novara, O. Zuffardi, G. Uziel, M. Zeviani, Severe X-linked mitochondrial encephalomyopathy associated with a mutation in apoptosis-inducing factor, Am. J. Hum. Genet 86 (2010) 639–649.
[22] C. Rinaldi, C. Grunseich, I.F. Sevrioukova, A. Schindler, I. Horkayne-Szakaly, C. Lamperti, G. Landoure, M.L. Kennerson, B.G. Burnett, C. Bonnemann, L.G. Biesecker, D. Ghezzi, M. Zeviani, K.H. Fischbeck, Cowchock syndrome is associated with a mutation in apoptosis-inducing factor, Am. J. Hum. Genet 91 (2012) 1095–1102.
[23] G. Sala, F. Trombin, S. Beretta, L. Tremolizzo, P. Presutto, M. Montopoli, M. Fantin, A. Martinuzzi, V. Carelli, C. Ferrarese, Antioxidants partially restore glutamate transport defect in leber hereditary optic neuropathy cybrids, J. Neurosci. Res. 86 (2008) 3331–3337.
[24] D. Vlachantoni, A.N. Bramall, M.P. Murphy, R.W. Taylor, X. Shu, B. Tulloch, T. Van Veen, D.M. Turnbull, R.R. McInnes, A.F. Wright, Evidence of severe mitochondrial oxidative stress and a protective effect of low oxygen in mouse models of inherited photoreceptor degeneration, Hum. Mol. Genet. 20 (2011) 322–335.
[25] C. La Morgia, M. Carbonelli, P. Barboni, A.A. Sadun, V. Carelli, Medical management of hereditary optic neuropathies, Front. Neurol. 5 (2014) 141.
[26] M. Vos, Esposito, J.N. Edirisinghe, S. Vilain, D.M. Haddad, J.R. Slabbaert, S. Van Meensel, O. Schaap, B. De Strooper, R. Meganathan, V.A. Morais, P. Verstreken, Vitamin K2 is a mitochondrial electron carrier that rescues pink1 deficiency, Science 336 (2012) 1306–1310.
[27] Y. Wen, W. Li, E.C. Poteet, L. Xie, C. Tan, L.J. Yan, X. Ju, R. Liu, H. Qian, M.A. Marvin, M.S. Goldberg, H. She, Z. Mao, S.H. Simpkins, S.H. Yang, Alternative mitochondrial electron transfer as a novel strategy for neuroprotection, J. Biol. Chem. 286 (2011) 16504–16515.
[28] N.L. Callaway, P.D. Riha, A.K. Bruchey, Z. Munshi, F. Gonzalez-Lima, Methylene blue improves brain oxidative metabolism and memory retention in rats, Pharmacol. Biochem. Behav. 77 (2004) 175–181.
[29] J.C. Rojas, J.M. John, J. Lee, F. Gonzalez-Lima, Methylene blue provides behavioral and metabolic neuroprotection against optic neuropathy, Neurotox. Res. 15 (2009) 260–273.
[30] A. Miclescu, S. Basu, L. Wiklund, Methylene blue added to a hypertonic-hyperoncotic solution increases short-term survival in experimental cardiac arrest, Crit. care Med. 34 (2006) 2806–2813.
[31] J.C. O'Leary 3rd, Q. Li, P. Marinec, L. Blair, E.E. Congdon, A.G. Johnson, U.K. Jinwal, J. Koren 3rd, J.R. Jones, C. Kraft, M. Peters, J.F. Abisambra, K.E. Duff, E.J. Weeber, J.E. Gestwicki, C.A. Dickey, Phenothiazine-mediated rescue of cognition in tau transgenic mice requires neuroprotection and reduced soluble tau burden, Mol. Neurodegener. 5 (2010) 45.
[32] J.C. Rojas, A.K. Bruchey, F. Gonzalez-Lima, Neurometabolic mechanisms for memory enhancement and neuroprotection of methylene blue, Prog. Neurobiol. 96 (2012) 32–45.
[33] L. Vutskits, A. Briner, P. Klauser, E. Gascon, A.G. Dayer, J.Z. Kiss, D. Muller, M.J. Licker, D.R. Morel, Adverse effects of methylene blue on the central nervous system, Anesthesiology 108 (2008) 684–692.

[34] N.L. Callaway, P.D. Riha, K.M. Wrubel, D. McCollum, F. Gonzalez-Lima, Methylene blue restores spatial memory retention impaired by an inhibitor of cytochrome oxidase in rats, Neurosci. Lett. 332 (2002) 83–86.
[35] D.X. Medina, A. Caccamo, S. Oddo, Methylene blue reduces abeta levels and rescues early cognitive deficit by increasing proteasome activity, Brain Pathol. 21 (2011) 140–149.
[36] S.Y. Shin, T.H. Kim, H. Wu, Y.H. Choi, S.G. Kim, SIRT1 activation by methylene blue, a repurposed drug, leads to AMPK-mediated inhibition of steatosis and steatohepatitis, Eur. J. Pharmacol. 727 (2014) 115–124.
[37] Y. Du, A. Veenstra, K. Palczewski, T.S. Kern, Photoreceptor cells are major contributors to diabetes-induced oxidative stress and local inflammation in the retina, Proc. Natl. Acad. Sci. USA 110 (2013) 16586–16591.
[38] Y. Jiang, R.J. Walker, T.S. Kern, J.J. Steinle, Application of isoproterenol inhibits diabetic-like changes in the rat retina, Exp. Eye Res. 91 (2010) 171–179.
[39] A. Burgess, S. Vigneron, E. Brioudes, J.C. Labbe, T. Lorca, A. Castro, Loss of human Greatwall results in G2 arrest and multiple mitotic defects due to deregulation of the cyclin B-Cdc2/PP2A balance, Proc. Natl. Acad. Sci. USA 107 (2010) 12564–12569.
[40] E. Tan, X.Q. Ding, A. Saadi, N. Agarwal, M.I. Naash, M.R. Al-Ubaidi, Expression of cone-photoreceptor-specific antigens in a cell line derived from retinal tumors in transgenic mice, Invest. Ophthalmol. Vis. Sci. 45 (2004) 764–768.
[41] P. Solinas, H. Fujioka, B. Tandler, C.L. Hoppel, Isolation of rat adrenocortical mitochondria, Biochem. Biophys. Res. Commun. 427 (2012) 96–99.
[42] L. Schild, S. Westphal, S. Scheithauer, M. Holfeld, W. Augustin, B.A. Sabel, Isolation of functionally intact pig retina mitochondria, Acta Ophthalmol. Scand. 74 (1996) 354–357.
[43] E.J. Vazquez, J.M. Berthiaume, V. Kamath, O. Achike, E. Buchanan, M.M. Montano, M.P. Chandler, M. Miyagi, M.G. Rosca, Mitochondrial complex I defect and increased fatty acid oxidation enhance protein lysine acetylation in the diabetic heart, Cardiovasc. Res. (2015).
[44] M.G. Rosca, E.J. Vazquez, J. Kerner, W. Parland, M.P. Chandler, W. Stanley, H.N. Sabbah, C.L. Hoppel, Cardiac mitochondria in heart failure: decrease in respirasomes and oxidative phosphorylation, Cardiovasc. Res. 80 (2008) 30–39.
[45] N. Apostolova, L.J. Gomez-Sucerquia, A. Moran, A. Alvarez, A. Blas-Garcia, J.V. Esplugues, Enhanced oxidative stress and increased mitochondrial mass during efavirenz-induced apoptosis in human hepatic cells, Br. J. Pharmacol. 160 (2010) 2069–2084.
[46] T.C. Nag, S. Wadhwa, Immunolocalisation pattern of complex I-V in ageing human retina: correlation with mitochondrial ultrastructure, Mitochondrion 31 (2016) 20–32.
[47] S. Wang, G. Birol, E. Budzynski, R. Flynn, R.A. Linsenmeier, Metabolic responses to light in monkey photoreceptors, Curr. Eye Res. 35 (2010) 510–518.
[48] G.A. Perkins, M.H. Ellisman, D.A. Fox, Three-dimensional analysis of mouse rod and cone mitochondrial cristae architecture: bioenergetic and functional implications, Mol. Vision. 9 (2003) 60–73.
[49] J.H. Kam, G. Jeffery, To unite or divide: mitochondrial dynamics in the murine outer retina that preceded age related photoreceptor loss, Oncotarget 6 (2015) 26690–26701.
[50] K. Kooragayala, N. Gotoh, T. Cogliati, J. Nellissery, T.R. Kaden, S. French, R. Balaban, W. Li, R. Covian, A. Swaroop, Quantification of oxygen consumption in retina Ex vivo demonstrates limited reserve capacity of photoreceptor mitochondria, Invest. Ophthalmol. Vis. Sci. 56 (2015) 8428–8436.
[51] D. Calzia, G. Garbarino, F. Caicci, L. Manni, S. Candiani, S. Ravera, A. Morelli, C.E. Traverso, I. Panfoli, Functional expression of electron transport chain complexes in mouse rod outer segments, Biochimie 102 (2014) 78–82.
[52] B.M. Kevany, K. Palczewski, Phagocytosis of retinal rod and cone photoreceptors, Physiology 25 (2010) 8–15.
[53] R.W. Young, The renewal of photoreceptor cell outer segments, J. Cell Biol. 33 (1967) 61–72.
[54] K. Palczewski, G protein-coupled receptor rhodopsin, Annu. Rev. Biochem. 75 (2006) 743–767.
[55] M.M. Humphries, D. Rancourt, G.J. Farrar, P. Kenna, M. Hazel, R.A. Bush, P.A. Sieving, D.M. Sheils, N. McNally, P. Creighton, A. Erven, A. Boros, K. Gulya, M.R. Capecchi, P. Humphries, Retinopathy induced in mice by targeted disruption of the rhodopsin gene, Nat. Genet. 15 (1997) 216–219.
[56] Y. Wen, W. Li, E.C. Poteet, L. Xie, C. Tan, L.J. Yan, X. Ju, R. Liu, H. Qian, M.A. Marvin, M.S. Goldberg, H. She, Z. Mao, J.W. Simpkins, S.H. Yang, Alternative mitochondrial electron transfer as a novel strategy for neuroprotection, J. Biol. Chem. 286 (2011) 16504–16515.
[57] J.M. Berthiaume, C.H. Hsiung, A.B. Austin, S.P. McBrayer, M.M. Depuydt, M.P. Chandler, M. Miyagi, M.G. Rosca, Methylene blue decreases mitochondrial lysine acetylation in the diabetic heart, Mol. Cell. Biochem. 432 (2017) 7–24.
[58] D.P. Narendra, S.M. Jin, A. Tanaka, D.F. Suen, C.A. Gautier, J. Shen, M.R. Cookson, R.J. Youle, PINK1 is selectively stabilized on impaired mitochondria to activate Parkin, PLoS Biol. 8 (2010) e1000298.
[59] X. Zheng, T. Hunter, Pink1, the first ubiquitin kinase, EMBO J. 33 (2014) 1621–1623.
[60] S.A. Sarraf, M. Raman, V. Guarani-Pereira, M.E. Sowa, E.L. Huttlin, S.P. Gygi, J.W. Harper, Landscape of the PARKIN-dependent ubiquitylome in response to mitochondrial depolarization, Nature 496 (2013) 372–376.
[61] F. Basit, L.M. van Oppen, L. Schockel, H.M. Bossenbroek, S.E. van Emst-de Vries, J.C. Hermeling, S. Grefte, C. Kopitz, M. Heroult, P. Hgm Willems, W.J. Koopman, Mitochondrial complex I inhibition triggers a mitophagy-dependent ROS increase leading to necroptosis and ferroptosis in melanoma cells, Cell Death Dis. 8 (2017) e2716.
[62] D. Narendra, A. Tanaka, D.F. Suen, R.J. Youle, Parkin is recruited selectively to impaired mitochondria and promotes their autophagy, J. Cell Biol. 183 (2008) 795–803.
[63] J.B. Lin, S. Kubota, N. Ban, M. Yoshida, A. Santeford, A. Sene, R. Nakamura, N. Zapata, M. Kubota, K. Tsubota, J. Yoshino, S.I. Imai, R.S. Apte, NAMPT-Mediated NAD(+) Biosynthesis Is Essential for Vision In Mice, Cell Rep. 17 (2016) 69–85.
[64] C.C. Alano, A. Tran, R. Tao, W. Ying, J.S. Karliner, R.A. Swanson, Differences among cell types in NAD(+) compartmentalization: a comparison of neurons, astrocytes, and cardiac myocytes, J. Neurosci. Res. 85 (2007) 3378–3385.
[65] L. Mouchiroud, R.H. Houtkooper, N. Moullan, E. Katsyuba, D. Ryu, C. Canto, A. Mottis, Y.S. Jo, M. Viswanathan, K. Schoonjans, L. Guarente, J. Auwerx, The NAD(+)/Sirtuin Pathway Modulates Longevity through Activation of Mitochondrial UPR and FOXO Signaling, Cell 154 (2013) 430–441.
[66] H. Zhang, D. Ryu, Y. Wu, K. Gariani, X. Wang, P. Luan, D. D'Amico, E.R. Ropelle, M.P. Lutolf, R. Aebersold, K. Schoonjans, K.J. Menzies, J. Auwerx, NAD(+) repletion improves mitochondrial and stem cell function and enhances life span in mice, Science 352 (2016) 1436–1443.
[67] G. Karamanlidis, C.F. Lee, L. Garcia-Menendez, S.C. Kolwicz Jr, W. Suthammarak, G. Gong, M.M. Sedensky, P.G. Morgan, W. Wang, R. Tian, Mitochondrial complex I deficiency increases protein acetylation and accelerates heart failure, Cell Metab. 18 (2013) 239–250.
[68] T.E. Akie, L. Liu, M. Nam, S. Lei, M.P. Cooper, OXPHOS-mediated induction of NAD + promotes complete oxidation of fatty acids and interdicts non-alcoholic fatty liver disease, PloS One 10 (2015) e0125617.
[69] W.J. Koopman, H.J. Visch, S. Verkaart, L.W. van den Heuvel, J.A. Smeitink, P.H. Willems, Mitochondrial network complexity and pathological decrease in complex I activity are tightly correlated in isolated human complex I deficiency, Am. J. Physiol. Cell Physiol. 289 (2005) C881–C890.